

# Polycaprolactone–thiophene-conjugated carbon nanotube meshes as scaffolds for cardiac progenitor cells

Abeni M. Wickham, Mohammad Mirazul Islam, Debasish Mondal, Jaywant Phopase, Veera Sadhu, Éva Tamás, Naresh Poliseti, Agneta Richter-Dahlfors, Bo Liedberg and May Griffith

**Linköping University Post Print**



N.B.: When citing this work, cite the original article.

Original Publication:

Abeni M. Wickham, Mohammad Mirazul Islam, Debasish Mondal, Jaywant Phopase, Veera Sadhu, Éva Tamás, Naresh Poliseti, Agneta Richter-Dahlfors, Bo Liedberg and May Griffith, Polycaprolactone–thiophene-conjugated carbon nanotube meshes as scaffolds for cardiac progenitor cells, 2014, Journal of Biomedical Materials Research. Part B - Applied biomaterials, (102), 7, 1553-1561.

<http://dx.doi.org/10.1002/jbm.b.33136>

Copyright: Wiley: 12 months

<http://eu.wiley.com/WileyCDA/>

Postprint available at: Linköping University Electronic Press

<http://urn.kb.se/resolve?urn=urn:nbn:se:liu:diva-111488>

# **Polycaprolactone-Thiophene Conjugated Carbon Nanotubes Meshes as Scaffolds for Cardiac Progenitor Cells**

Abeni M Wickham<sup>a,†</sup>, M Mirazul Islam<sup>b,c,†</sup>, Debasish Mondal<sup>a,†</sup>, Jaywant Phopase<sup>a</sup>, Veera Sadhu<sup>a</sup>,  
Éva Tamás<sup>d</sup>, Naresh Poliseti<sup>c</sup>, Agneta Richter-Dahlfors<sup>b</sup>, Bo Liedberg<sup>a,e</sup>, May Griffith<sup>b,c</sup>

<sup>a</sup> Integrative Regenerative Medicine (IGEN) Centre and Dept. of Physics, Chemistry and Biology, Linköping University, Linköping Sweden

<sup>b</sup> Swedish Medical Nanoscience Centre, Department of Neuroscience, Karolinska Institutet, Stockholm, Sweden

<sup>c</sup> Integrative Regenerative Medicine (IGEN) Centre and Dept. of Clinical and Experimental Medicine, Linköping University, Linköping Sweden

<sup>d</sup> Division of Cardiovascular Diseases, Dept. of Medicine and Health Sciences, Linköping University, Sweden; and Dept. of Cardiothoracic Surgery UHL, County Council of Östergötland, Linköping, Sweden

<sup>e</sup> Centre for Biomimetic Sensor Science, Nanyang Technological University, Singapore

<sup>†</sup> Equivalent contribution

## **Corresponding author:**

May Griffith, PhD

E-mail: [may.griffith@liu.se](mailto:may.griffith@liu.se)

Phone number: (+46) 13 28 17 56

Fax number: (+46) 10 103 42 73

## **Abstract**

The myocardium is unable to regenerate itself after infarct, resulting in scarring and thinning of the heart wall. Our objective was to develop a patch to buttress and bypass the scarred area, while allowing regeneration by incorporated cardiac stem/progenitor cells (CPCs). Polycaprolactone (PCL) was fabricated as both sheets by solvent casting, and fibrous meshes by electrospinning, as potential patches, to determine the role of topology in proliferation and phenotypic changes to the CPCs. Thiophene-conjugated carbon nanotubes (T-CNT) were incorporated to enhance the mechanical strength. We showed that freshly isolated CPCs from murine hearts did not attach nor spread on the PCL sheets, both with and without T-CNT. As electrospun meshes, however, both PCL and PCL/T-CNT supported CPC adhesion, proliferation and differentiation. The incorporation of T-CNT into PCL resulted in a significant increase in mechanical strength but no morphological changes to the meshes. In turn, proliferation, but not differentiation, of CPCs into cardiomyocytes was enhanced in T-CNT containing meshes. We have shown that changing the topology of PCL, a known hydrophobic material, dramatically altered its properties, in this case, allowing CPCs to survive and differentiate. With further development, PCL/T-CNT meshes or similar patches may become a viable strategy to aid restoration of the post-MI myocardium.

**Keywords:** *Topology, carbon nanotubes, polycaprolactone, cardiac progenitor cells, electrospun meshes.*

**Running Head:** PCL/CNT scaffolds for cardiac progenitor cells

## **Introduction**

The WHO estimates that heart failure due mainly to myocardial infarction (MI) accounts for about 29% of deaths worldwide [1]. While regenerative medicine has generated a lot of hope due to high impact preclinical reports, e.g. direct reprogramming of non-muscle heart cells to form muscle in mice [2], most studies deal with early intervention and re-establishment of vasculature to the heart. However, many patients do not make it to the hospital in time, and scarring of the left ventricle (most common place of infarct) occurs, leaving a large scarred, dilated and thinned heart wall (Fig. 1) that decreases the heart's pumping capacity. In fact, upon MI, a patient can lose as much as 50 grams of muscle mass, as a result of hypoxia that leads to the release of apoptotic factors and cell death. Studies have shown that cell implantation can improve clinical function, but do better with a scaffold to provide a 3-dimensional framework to direct the organization of cells into functional tissue and organs [3]. Although removal of the scar tissue and replacement with a suitable cellular construct would be ideal to restore contractile function, this is somewhat unrealistic in the near future.

Our objective was to develop a patch comprising biocompatible materials and incorporated cardiac stem/progenitor cells (CPCs) that can be used to reinforce and bridge the damaged area, so that the thin, dilated heart wall is strengthened (Fig. 1). The incorporation of CPCs (or an appropriate progenitor) will allow formation of new myocardial tissue and hence a more permanent by-pass. The human myocardium is a very tough tissue, and therefore any patch has to be strong enough to withstand the high pressures exerted with each heartbeat and volume of blood flowing through.

In this study, polycaprolactone (PCL), a US FDA approved polyester commonly used in biomedical applications [4-8] was selected as a model biomaterial for the potential patch. We

compared the effects of changing the physical properties of PCL sheets by augmenting the mechanical strength using carbon nanotubes (CNTs.) We also examined the effects of a change in topology from a PCL sheet to a mesh conformation on the growth and differentiation characteristics of CPCs. CNTs were chosen as they have been incorporated into polymer fibers [9], including electrospun materials [10, 11] and have been reported to greatly enhance their strength. Conjugated CNTs allow for better solubility as pristine CNTs can interact via van der Waals forces and aggregate [12]. There are many ways to conjugate CNTs for improved solubility, but the majority lead to significant changes in the chemical composition and behaviour of the material [13, 14]. Thiophene conjugation of the CNTs in this study had little/no effect on mesh fabrication, while augmenting the mechanical strength of the composite material without other undesired effects.

## **2. Materials and Methods**

### **2.1. Materials**

All chemicals and reagents were purchased from Sigma-Aldrich (St. Louis, USA) unless otherwise specified. The carbon nanotubes (CNTs) used were all multi-walled CNTs from Sigma, 7-15 nm in diameter, that were produced by a variant of the standard arc discharge evaporation of carbon, resulting in CNT deposition at the negative cathode.

### **2.2 Preparation of PCL and PCL/T-CNT**

Thiophene-conjugated carbon nanotubes (T-CNTs) were synthesized as described in Sadhu et al. [15] to a final concentration of 1mg/mL. After thiophene conjugation, the T-CNTs were 7-15 nm in diameter and 2  $\mu$ m in length [15]. PCL pellets were dissolved in chloroform to give a 10% w/w solution. For T-CNT doped PCL, T-CNTs were dispersed by ultrasonication and added to the PCL

solution at a ratio of PCL/CNT of 1.0:0.2 (w/w). Finally, the suspension was ultrasonicated for another one hour and then stirred continuously before casting and electrospinning.

### **2.3. Casting PCL sheets**

PCL and PCL/T-CNT in the 10% chloroform solutions were cast on glass slides at room temperature. The solvent was left to evaporate slowly over two days, leaving a flat film.

### **2.4. Electrospinning Fibrous Meshes**

Solutions of PCL or PCL/T-CNT (PCL/T-CNT ratio of 1.0:0.2) were fed into a 2 ml standard syringe attached to a 23 G blunted stainless steel needle using a syringe pump (Chemyx, TX, USA) at a flow rate of  $0.5 \text{ ml h}^{-1}$  with an applied voltage (Glassman High Voltage Inc., NJ, USA) of 6.2 kV. On application of high voltage the polymer solution was drawn into fibers and collected on collector plate wrapped with aluminum foil, kept at a distance of 15 cm from the needle tip. These fibers were dried overnight under vacuum to completely remove solvent residue prior to use for characterization and cell culture studies.

### **2.5. Characterization of the fibrous meshes**

#### *2.5.1. Scanning electron microscopy*

PCL only sheets and meshes were sputter coated with chromium and imaged by scanning electron microscopy (SEM), using an accelerative voltage of 5kV (LEO 1550 Gemini). The electrospun PCL and composite PCL/T-CNTs fibrous meshes were sputter coated with gold and imaged at an accelerating voltage of 10kV using the SEM (JEOL JSM-840).

#### *2.5.2. Mechanical properties*

The mechanical properties of PCL and PCL/T-CNT fibrous meshes were tested using an Instron® universal test machine (ElectroPuls E3000, High Wycombe, UK) in a water bath conditioned at 37°C. The samples were trimmed to the dimensions of 26 x 8 mm. The mean thickness of each

sample was 0.130 mm, and the distance between the gripping points was 15-16 mm. The mechanical testing was conducted with the grips moving at a stretch speed of 10 mm/min and a load cell of 50 N. The data acquisition ratio was set to 20.0 Hz. The reported data on tensile strength and elongation represent the average results of five tests. The tensile strength was calculated from the load vs. extension curves using the Bluehill® software.

### *2.5.3 Contact angle wettability studies*

Contact angle measurements were made using the sessile drop technique. Drops of water were deposited onto the PCL and PCL/T-CNT sheets. The static angles were imaged and calculated with a CAM 200 Optical Contact Angle Meter (KSV Instruments Ltd, Finland).

## **2.6. In vitro cell studies**

### *2.6.1. Isolation of cardiac progenitor cells (CPCs)*

Cardiac progenitor cells (CPCs) were freshly isolated from 3-week-old C57BL/6 mouse hearts using a Millipore Cardiac Stem Cell Isolation kit (Millipore, Darmstadt, Germany), following the manufacturer's protocol and with prior ethical approval from the Djurförsöksetiska nämnden Linköping (animal ethical committee). After isolation, cells were cultured in CPC maintenance medium consisting of DMEM/Ham F12 medium supplemented with 10% FCS, 1% antibiotic and antimycotic solution (Invitrogen Corp, USA), 1X ITS (Insulin-Transferrin-Selenium) (GIBCO, Life Technologies, Darmstadt, Germany) and 0.5% DMSO, 20ng/ml Epidermal Growth Factor. Cells were incubated at 37 °C in a humidified atmosphere containing 5% CO<sub>2</sub> for 6 days, and the culture medium was changed once every 2 days. Their identity as CPCs was confirmed by Fluorescent Associated Cell Sorting (FACS) Analysis using different markers (Table 1). Briefly, single cell suspensions of  $0.5 \times 10^6$  cells (passage 2) were suspended in 100 µl of PBS containing 0.2% sodium azide and 2% fetal calf serum (FCS), and then incubated on ice in the dark for 30

minutes in saturated concentrations of their respective antibodies. They were washed three times by centrifuging at 200 x g for 5 minutes, followed by suspension in cold PBS. Cell fluorescence was evaluated by flow cytometry by using a Gallios multicolour flow cytometer (Beckman Coulter AB, Sweden). The data was analyzed using Kluza software (BD, San Jose, CA). An isotype control of each antibody was included in the experiment and positivity for a particular antibody was measured from the cross point of the isotype and corresponding antibody graph. A total of 10,000 events were acquired to determine the positivity of different markers.

#### *2.6.2. Cardiac progenitor cell culture on sheets and meshes*

Round, 9 mm diameter samples of sheets and meshes were trephined out and placed in a 24-well culture dish, and washed overnight in PBS containing a 1% penicillin-streptomycin (PEST) solution, after which the antibiotic solution was rinsed off. CPCs were then seeded onto the scaffolds at a density of  $1 \times 10^4$  cells/well and maintained in CPC maintenance medium at 37°C in a humidified incubator at 5% CO<sub>2</sub>. To allow differentiation, CPCs ( $1 \times 10^4$  cells) were seeded onto the scaffolds and incubated in maintenance medium for one day to allow them to attach. The next day, the medium was changed to the induction medium for CPC differentiation and the samples were cultured for an additional 72 hours. The induction medium consisted of DMEM/Ham's F12 medium with 15mM HEPES supplemented with 10µM 5'-azacytidine, 1% FCS, 1% PEST, 1X ITS and 0.5% DMSO. The medium was then changed to cardiomyocyte maintenance medium which comprised DMEM/Ham's F12 with 15mM HEPES supplemented with 1% FCS, 1% PEST, 1X ITS, 0.5% DMSO, 20ng/ml EGF and 10ng/ml TGF-β1 and maintained for 21 days by changing medium every alternate day.

### *2.6.3. Cell viability and proliferation assays*

Viability of CPCs on their scaffolds was assessed on days 1 and 7 of culture using a Live/Dead® Viability/Cytotoxicity Kit (L3224, Life Technologies, Darmstadt, Germany). Cell adhesion and proliferation on the meshes (cells on sheets were non-viable) were determined using the colorimetric MTS assay (CellTiter 96 AQueous One solution, Promega, Madison, WI, USA). At days 1, 4, and 7 of culture, cell-seeded meshes were transferred clean 24-well plates after removing the medium at different specific time points. Samples were rinsed with PBS to remove unattached cells and incubated with 20% MTS reagent in a cell culture medium for a period of 4 hours at 37 °C. Absorbance of the obtained dye was measured at 490 nm using a spectrophotometric microplate reader (VERSA Max Microplate Reader, Molecular Devices, Berkshire, UK). A standard curve was prepared using known numbers of cells. From this, we obtained the cell numbers for each time point and sample [29].

### *2.6.4. Immunofluorescence*

CPCs grown on meshes were characterized by immunofluorescence for cardiac stem/progenitor specific markers, and after 21 days of culture after differentiation induction, with cardiomyocyte markers. Briefly, cells within meshes were rinsed thoroughly with PBS and fixed with 4% paraformaldehyde for 20 minutes. For permeabilization and blocking unspecific binding, samples were incubated with 3.0% bovine serum albumin (BSA) with 0.30% Triton X-100 in PBS for 45min at 37°C. Samples were then incubated with primary antibodies diluted in blocking buffer as given in Table 2. After application of primary antibodies, samples were rinsed and then reacted with their respective secondary antibodies (Table 2). The samples were counterstained with DAPI (4', 6-diamidino-2-phenylindole, dihydrochloride) for one minute and mounted using 50% (v/v) glycerol in PBS.

Controls consisted of omission of the primary antibody and substitution of either mouse or rabbit IgG. Stained samples were visualized by laser confocal microscopy.

## **2.7. Statistical Analysis**

Mean values were obtained. Statistical analyses were performed using a Generalized Linear Model (GLM, Minitab Statistical Software, Minitab Ltd., Coventry, UK).

## **3. Results**

### **3.1. PCL and PCL/T-CNT sheets and meshes**

SEM showed that both PCL and PCL/T-CNT sheets were two dimensional with a small surface area (Fig. 2A,B). They were hydrophobic and not cell friendly (see below). Both PCL and PCL/T-CNT were readily electrospun into fibrous meshes. Unlike the sheets, these meshes were 3-dimensional, porous structures. No obvious morphological differences were observed between the PCL only and T-CNT containing electrospun PCL meshes by SEM (Fig. 2C, D). However, there were significant differences in the mechanical properties of PCL meshes after the addition of T-CNT to the PCL (Table 3). The addition of the T-CNT increased the tensile strength from 0.9 to 1.3 MPa, and elongation at break by over 2.5 fold, from 48% elongation at break to 131%.

### **3.2. Cardiac Progenitor Cells and Growth Characteristics on Materials**

FACS analyses (Fig. 3) showed that the cells isolated from murine hearts were 97% Sca-1 positive, 24% positive for CD34 and 78% positive for GATA-4, a cardiac progenitor lineage specific marker. These cells were 100% and 96% positive for mesenchymal stem cell specific surface antigens, CD 29 and CD 44 respectively. The cells were negative for hematopoietic lineage specific markers, APC cocktail lineage, and for the vascular endothelial marker, CD31. These results confirmed the identity of the cells isolated from murine hearts as CPCs.

When seeded onto sheets of either PCL only or PCL/T-CNT, the majority of the cells died within 1 day (Fig 4A, B). However, with a change in topology to the electrospun meshes, most cells remained viable (Fig 4C-F).

The MTS assays showed that cells remained viable but did not increase in numbers during the first four days in culture (Fig. 5). GLM calculations gave a  $p > 0.05$  for the materials, the day and the crossed factor. The Tukey test showed a significant overall difference amongst the materials. Growth of control cells seeded on tissue culture plastic was continuous, without the lag time seen on the meshes. This lag was seen to yield no significant difference at day 4 between the PCL and PCL/T-CNT meshes. However, by day 7 there is a significant difference in cell growth for both meshes and the control ( $p < 0.0001$ ).

### **3.3. Effect of PCL and PCL/T-CNT Substrates on Cardiac Progenitor Phenotype**

The ability of the CPCs to retain their phenotypes on the meshes was demonstrated by their expression of smooth muscle actin, c-kit, and Isl-1 at both day 4 and 7 of cell culturing (Fig 6). There was a marked increase in the number of actin, c-kit, and Isl-1 stained cells on the PCL/T-CNT meshes in comparison to the PCL only meshes, on day 7 in particular.

When the CPCs were induced to differentiate, they expressed markers of differentiated cardiomyocytes such as  $\alpha$ -actinin, atrial natriuretic peptide (ANP) and cardiomyocyte myosin heavy chain (MHC). There was no observable difference in the numbers of cells on PCL/T-CNT or PCL only meshes that expressed  $\alpha$ -actinin, ANP or MHC (Fig 7). None of the cells showed the typical morphology of fully differentiated cardiomyocytes. There were no identifiable sarcomeres, which would have been visible with  $\alpha$ -actinin staining. It was noted that tissue culture plastic seeded CPCs, although higher in numbers, did not show terminal differentiation either.

#### 4. Discussion

Thiophene-conjugated CNTs were readily incorporated into PCL, which in turn could be cast into sheets as well as electrospun. Two-dimensional sheets of either PCL alone or T-CNT containing PCL were not cell friendly, in agreement with previous reports of it as a hydrophobic polymer with little biological activity [12,30]. In this study, PCL sheets did not support CPC growth at all, nor did addition of the T-CNT to PCL improve biocompatibility.

Topography has been reported to be important for cellular behavior, with a growing consensus that an increased surface area is necessary for cell adhesion and proliferation [4,6]. The difference between a 2D environment and 3D environment is clear from our results. It is most likely that the 3D porous fibrous meshes were entrapping cell culture media macromolecules within the pores needed for the cells to be viable, proliferate and differentiate, while the 2D flat sheets did not allow retention of media components.

The addition of T-CNT to the PCL meshes via electrospinning also resulted in an increase in mechanical stability of the materials, particularly in their elasticity as shown by the over 2.5-fold increase in the percent elongation at break. This increase in mechanical strength has also been reported for other polymer/CNT composites with PCL, polycarbonate, polyurethane, and chitosan [31-34], showing the utility of CNT as a means for mechanically enhancing the strength of biomaterials. This was the only change that was experimentally evident, as even the wettability of PCL and PCL/T-CNT sheets are similar at  $76 \pm 1.1$  and  $77 \pm 0.9$  for the PCL and PCL/T-CNT respectively.

Although both PCL and PCL/T-CNT meshes supported CPC attachment, proliferation was enhanced on the PCL/T-CNT meshes. The lag time seen on the meshes has been reported before [35] and bears no indication of effect from the materials. As the topography of PCL and PCL/T-

CNT meshes was similar, the difference in rate of cell proliferation was most likely due to the difference in the mechanical properties of the two meshes. The stronger PCL/T-CNT meshes also supported better retention of the CPC phenotype (expression of c-kit and Isl-1 in particular) during the proliferative phase. The higher rate of proliferation and expression of cardiac progenitor markers is probably due to the difference in mechanical properties, and in particular, the increased elasticity.

After induction of differentiation, the cells expressed specific markers of differentiated cardiomyocytes such as  $\alpha$ -actinin, ANP and cardiomyocyte MHC. There was no statistical difference in the numbers of cells that expressed  $\alpha$ -actinin, ANP, and MHC between the PCL/T-CNT and PCL only meshes. In these simple cultures, terminal morphological differentiation of CPCs into myocardial cells with banding, e.g. Z-lines, was not achieved even though  $\alpha$ -actinin, which is involved in formation and maintenance of the Z-lines, was present. Nevertheless, we have shown the potential for the meshes to support cardiomyocyte differentiation from CPCs.

Unlike in the case of previous studies [36,37], the functionalization of the CNT, in this case with thiophenes, appears to have a very limited or pasive role in the differentiation of the CPCs. More importantly, however, PCL/T-CNT meshes were conducive to CPC proliferation with retention of the CPC phenotype, and they allowed differentiation and acquisition of cardiomyocyte markers.

## **5. Conclusions**

We have shown that changing the topological conformation of PCL, a known hydrophobic material, considerably altered its properties. The incorporation of T-CNT enhanced the mechanical properties of the fibrous meshes without changing its topography. The electrospun 3D PCL/T-

CNT meshes were conducive as scaffolds for CPCs to proliferate and differentiate. With further development, such meshes may in the future be viable as patches to aid restoration of cardiac function after MI, by buttressing and bypassing the scarred areas.

### **Acknowledgements**

MG & BL thank the Swedish Research Council and AFA Försäkring for grant support. The authors would like to thank Joel Edin for assistance with the statistical analyses.

### **References**

1. World Health Organization, Cardiovascular diseases (CVDs), Fact sheet N°317, September 2011.
2. Qian L, Huang J, Spencer I, Foley A, Vedantham V, Liu L, Conway S.J, Fu J-D, Srivastava D. *In vivo* reprogramming of murine cardiac fibroblasts into induced cardiomyocytes. *Nature* 2012; 485: 593-598.
3. Venugopal JR, Prabhakaran MP, Mukherjee S, Ravichandran R, Dan K, Ramakrishna S. Biomaterial strategies for alleviation of myocardial infarction. *J. R. Soc. Interface* 2012; 9: 1–19.
4. Ross A.M, Jiang Z, Bastmeyer M, Lahann J. Physical aspects of cell culture substrates: Topography, roughness, and elasticity. *Small* 2011; 8: 1-20.
5. Murtuza B, Nichol J.W, Khademhosseini A. Micro- and nanoscale control of the cardiac stem cell niche for tissue fabrication. *Tissue Eng Part B Rev* 2009; 15: 443-454.
6. Chen C.S, Mrksich M, Huang S, Whitesides G.M, Ingber D.E. Geometric control of cell life and death. *Science* 1997; 276: 1425-1428.
7. Nair L.S, Laurencin C. T. Biodegradable polymers as biomaterials. *Prog. Polym. Sci.* 2007; 32 : 762–798.

8. Woodruff M.A, Hutmacher D. W. The return of a forgotten polymer—Polycaprolactone in the 21st century. *Progress in Polymer Science* 2010; 35: 1217–1256.
9. Baughman R.H, Zakhidov A.A, de Heer W.A. Carbon nanotubes- the route toward applications. *Science* 2002; 297: 787-792.
10. Moniruzzaman M, Winey K.I. Polymer nanocomposites containing carbon nanotubes." *Macromolecules* 2006; 39: 5194-5205.
11. Coleman J.N, Khan U, Gun'ko Y.K. Mechanical reinforcement of polymers using carbon nanotubes. *Adv Mat* 2006; 18: 689–706.
12. Zou J, Liu L, Chen H, Khondaker S.I, McCullough R.D, Huo Q, Zhai L. Dispersion of pristine carbon nanotubes using conjugated block copolymers. *Adv Mat* 2008; 20: 2055–2060.
13. Yi C, Qi S, Zhang D, Yang M. Covalent conjugation of multi-walled carbon nanotubes with proteins. *Methods Mol Biol* 2010; 625: 9-17.
14. Khandare J.J, Jalota-Badhwar A, Satavalekar S. D, Bhansali S.G, Aher N.D, Kharas F, Banerjee S.S. PEG-conjugated highly dispersive multifunctional magnetic multi-walled carbon nanotubes for cellular imaging. *Nanoscale* 2012; 4: 837-844.
15. Sadhu V, Nismy N.A, Adikaari A.A.D.T, Henley S.J, Shkunov M, Silva S.P. The incorporation of mono- and bi-functionalized multiwall carbon nanotubes in organic photovoltaic cells. *Nanotechnology* 2011; 22: 1-5.
16. Matsuura K, Nagai T, Nishigaki N, Oyama T, Nishi J, Wada H, et al. Adult cardiac Sca-1 positive cells differentiate into beating cardiomyocytes. *J Biol Chem* 2004; 279: 11384-11391.

17. Asahara T, Murohara T, Sullivan A, Silver M, van der Zee R, Li T, et al. Isolation of putative progenitor endothelial cells for angiogenesis. *Science* 1997; 275: 964-967.
18. Grepin C, Robitaille L, Antakly T, Nemer M. Inhibition of transcription factor GATA-4 expression blocks in vitro cardiac muscle differentiation. *Mol Cell Biol* 1995; 15: 4095-4102.
19. Yang M-C, Chi N-H, Chou N-K, Huang Y-Y, Chung T-W, Chang Y-L, et al. The influence of rat mesenchymal stem cells CD44 surface markers on cell growth, fibronectin expression, and cardiomyogenic differentiation on silk fibroin- hyaluronic acid cardiac patches. *Biomaterials* 2010; 31: 854-862.
20. Bayes-Genis A, Soler-Botija C, Farre J, Sepulveda P, Raya A, Roura S, et al. Human progenitor cells derived from cardiac adipose tissue ameliorate myocardial infarction in rodents. *J Mol Cell Cardiol.* 2010; 49: 771-780.
21. Foudi A, Hochedlinger K, Van Buren D, Schindler JW, Jaenisch R, Carey V, Hock H. Analysis of histone 2B-GFP retention reveals slowly cycling hematopoietic stem cells. *Nat Biotech.* 2009; 27: 84-90.
22. Reyes M, Dudek A, Jahagirdar B, Koodie L, Marker PH, Verfaillie CM. Origin of endothelial progenitors in human postnatal bone marrow. *J Clin Invest.* 2002; 109: 337-346.
23. Skalli O, Pelte MF, Peclet MC, Gabbiani G, Bussolati G, Ravazzola M, Orci L. Alpha-smooth muscle actin, a differentiation marker of smooth muscle cells, is present in microfilamentous bundles of pericytes. *J Histochem Cytochem* 1989; 37: 315-321.

24. Fazel S, Cimini M, Chen L, Li S, Angoulvant D, Fedak P, Verma S, et al. Cardioprotective c-kit<sup>+</sup> cells are from the bone marrow and regulate the myocardial balance of angiogenic cytokines. *J Clin Invest* 2006; 116: 1865-1877.
25. Bu L, Jiang X, Martin-Puig S, Caron L, Zhu S, Shao Y, et al. Human Isl-1 heart progenitor generate diverse multipotent cardiovascular cell lineages. *Nat Let* 2009; 460: 113-118.
26. Jackson KA, Majka SM, Wang H, Pocius J, Hartley CJ, Majesky MW, et al. Regeneration of ischemic cardiac muscle and vascular endothelium by adult stem cells. *J Clin Invest.* 2001; 107:1395-1402.
27. Magga J, Vuolteenaho O, Tokola H, Marttila M, Ruskoaho H. B-type natriuretic peptide: a myocyte-specific marker for characterized load-induced alterations in cardiac gene expression. *Ann Med* 1998; 30: 39-45.
28. Arsic N, Mamaeva D, Lamb NJ, Fernandez A. Muscle-derived stem cells isolated as non-adherent population give rise to cardiac, skeletal muscle and neural lineages. *Exp cell Res.* 2008; 314:1266-1280
29. Halbleib M, Skurk T, Luca C, Heimburg D, Hauner H. Tissue engineering of white adipose tissue using hyaluronic acid-based scaffolds. I: in vitro differentiation of human adipocyte precursor cells on scaffolds. *Biomaterials* 2003; 24: 3125–3132
30. Tang Z.G, Black R.A, Curran J.M, Hunt, J.A, Rhodes N.P, Willams D.F. Surface properties and biocompatibility of solvent-cast poly[e-caprolactone] films. *Biomaterials* 2004; 25: 4741–4748.
31. Saeed K, Park S.Y, Ishaq M. Adsorption of multiwalled carbon nanotube on electrospun polycaprolactone nanofibers *J. Chil Chem. Soc.* 2009; 54: 375-378.

32. Mukherjee M, Das T, Rajasekar R. Bose S, Kumar S. Das C.K. Improvement of the properties of PC/LCP in the presence of carbon nanotubes. *Comp Part A* 2009; 40: 1291-1298.
33. Kuan H.C, Ma C.C.M, Chang W.P, Yuen S.M, Wu H.H, Lee T.M. Synthesis, thermal, mechanical and rheological properties of multiwall carbon nanotube/waterbourne polyurethane Nano composite. *Compos Sci Tech* 2005; 65: 1703-1710.
34. Azeez A.A, Rhee K.Y, Park S.J, Kim H.J, Jung D.H. Application of cryomilling to enhance material properties of carbon nanotube reinforced chitosan nanocomposite. *Compos Part B* 2013; 50: 127-134.
35. Gonzalez A, Rota M, Nurzynska D, Misao Y, Tillmanns J, Ojaimi C, et al. Activation of cardiac progenitor cells reverses the failing heart senescent phenotype and prolongs lifespan. *Circ Res* 2008;102: 597-606.
36. Nayak T.R, Jian L, Phua L.C, Ho H.K, Ren Y, Pastorin G. Thin films of functionalized multiwalled carbon nanotubes as suitable scaffold materials for stem cell proliferation bone formation. *ACS Nano* 2010; 4: 7717-7725.
37. Correa-Duarte M.A, Wagner N, Rojas-Chapana J, Morscheck C, Thie M, Giersig M. Fabrication and biocompatibility of carbon nanotube-based 3D networks as scaffold for cell seeding and growth. *Nanoletters* 2004; 4: 2233-2236.

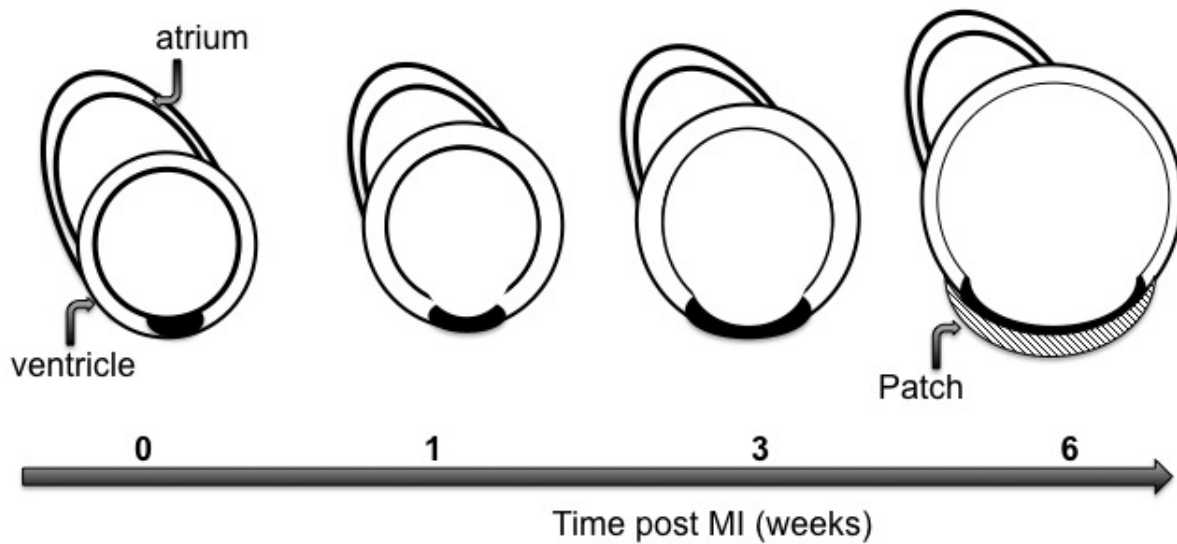


Figure 1.

Figure 1. Diagram showing development of ventricular scarring and dilation after MI, and position of proposed patch.

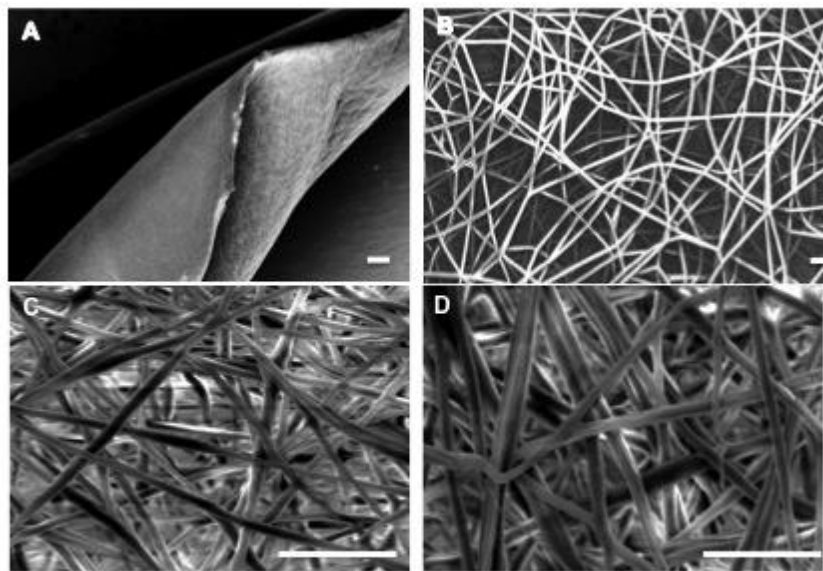


Figure 2.

Figure 2. SEM images showing topological difference between A) PCL sheets and B) PCL fibers. Scale bar 20 $\mu$ m. The incorporation of thiophene-conjugated carbon nanotubes (T-CNT) did not alter the morphology of the meshes, as seen in SEM micrographs of electrospun PCL (C) and PCL/T-CNT (D) fibrous meshes. Scale bar, 10 $\mu$ m.

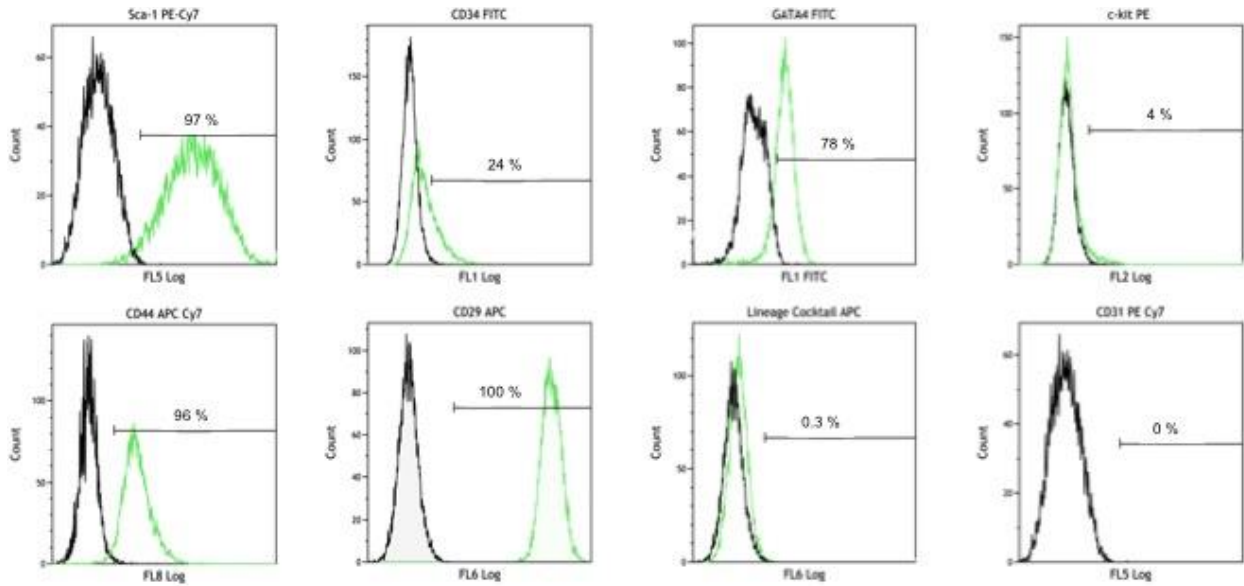


Figure 3.

Figure 3. Expression of stem cell markers (sca-1, c-kit, CD34), cardiac specific marker (GATA-4), stromal markers (CD44, CD29), haematopoietic marker (Cocktail lineage APC), endothelial marker (CD31) along with isotype controls on CPCs by FACS analysis. The black and green curves represent the expression of isotype control and specific markers, respectively.

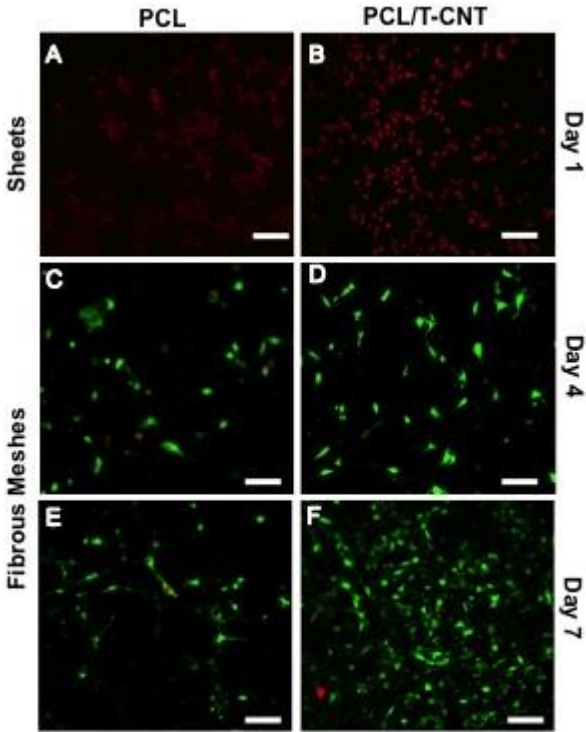


Figure 4.

Figure 4. CPC viability on (A, B) PCL sheets on day 1; (C, E) PCL and PCL/T-CNT meshes at day 4 respectively; and (D,F) PCL and PCL/T-CNT meshes on day 7. Scale bar, 50µm.

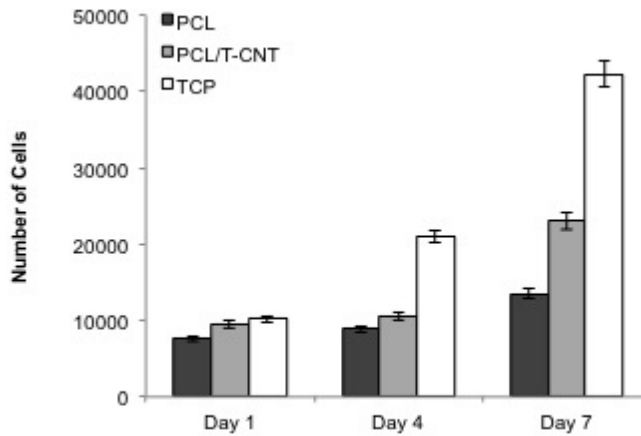


Figure 5.

Figure 5. Proliferation of CPCs on PCL, PCL/T-CNT, and tissue culture plastic (TCP) at days 1, 4 and 7 of culture, as determined using the MTS assay. Cell numbers were plotted by comparison with a standard curve established with known numbers of cells.

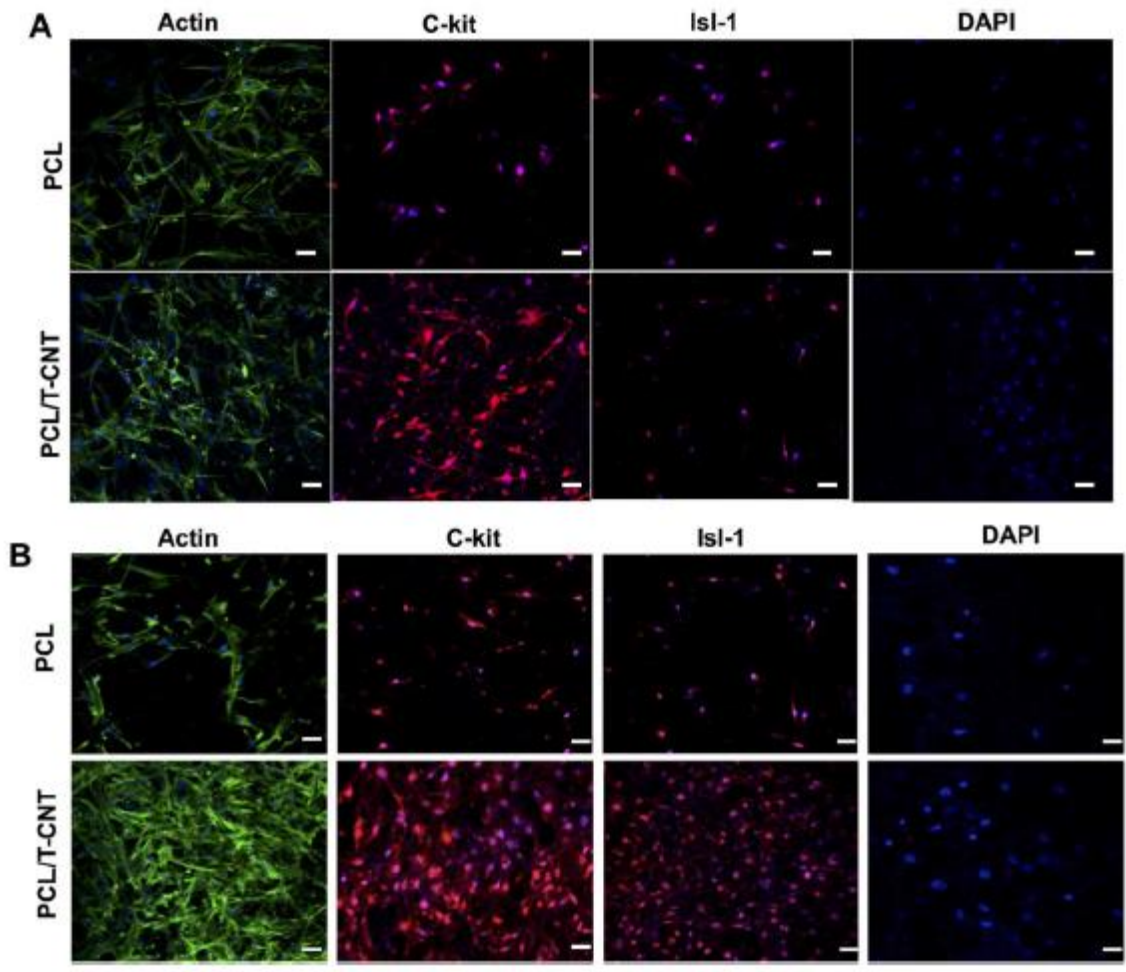


Figure 6. Immunofluorescent staining of CPCs seeded on PCL and PCL/T-CNT meshes, showing the expression of cardiac specific stem/progenitor cell makers - actin, c-kit, and Isl-1 at day 4 (A), and day 7 (B) of culture. The DAPI stained cell nuclei show the presence of more cells on the T-CNT containing meshes. Scale bar, 50 $\mu$ m.

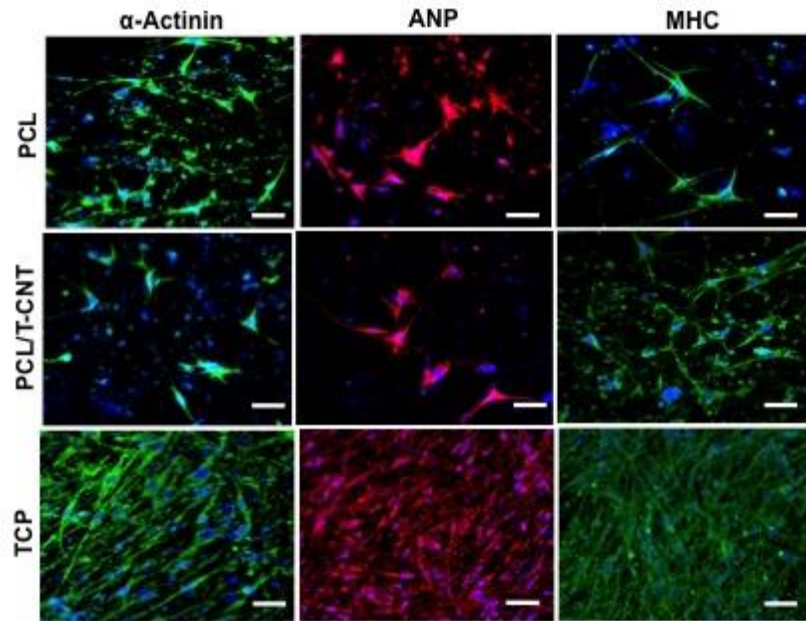


Figure 7.

Figure 7. Expression of cardiomyocyte markers,  $\alpha$ -actinin, atrial natriuretic peptide (ANP) and myosin heavy chain (MHC) in CPCs that have been induced to differentiate 21 days after seeding onto PCL or PCL-T-CNT meshes, or tissue culture plastic (TCP). Scale bar, 50 $\mu$ m.

**Table 1.** Antibodies used for Fluorescence Activated Cell Sorting analysis of cardiac progenitor cells.

<b>Primary Antibodies for FACS</b>					
<b>Abbrev.</b>	<b>Antigen</b>	<b>Marker of</b>	<b>Clone</b>	<b>Supplier</b>	<b>Ref</b>
Sca-1-PE-cy7	Lymphocyte 6A-2/6E-1	Hematopoietic stem cells	D7	BD Pharmingen, NJ, USA	[16]
CD34-FITC	Mouse CD34	Hematopoietic stem cells	RAM34	BD Pharmingen, NJ, USA	[17]
GATA4	Gata binding protein 4	Cardiac muscle cells	L97-56	BD Pharmingen, NJ, USA	[18]
CD44-APC-cy7	CD44 glycoprotein	Mesenchymal stem cells	IM7	BD Pharmingen, NJ, USA	[19]
CD29-APC	Integrin $\beta_1$ chain	Mesenchymal stem cells	MAR4	BD Pharmingen, NJ, USA	[20]
Cocktail lineage-APC	CD3e, CD11b, CD45R/B220, Ly-76, Ly-6G, and Ly-6C	Hematopoietic stem cells	145-2C11, M1/70, RA3-6B2, TER-119, and RB6-8C5	BD Pharmingen, NJ, USA	[21]
CD31-PE-cy7	Platelet endothelial cell adhesion molecule	Mature endothelial cells	390	BD Pharmingen, NJ, USA	[22]

**Table 2.** Antibodies used for immunofluorescent visualization of markers for cardiac progenitor cells and differentiating cardiomyocytes.

<b>Primary Antibodies for Immunofluorescence</b>						
<b>Abbrev.</b>	<b>Antigen</b>	<b>Marker of</b>	<b>Clone</b>	<b>Dilution</b>	<b>Supplier</b>	<b>Ref</b>
Anti-actin	Alpha smooth muscle actin	Smooth muscle	1A4	1/100	Abcam, Cambridge, UK	[24]
C-kit	CD11 or protooncogene C-kit	Hematopoietic stem cells/ adult cardiac stem cells	104D2	1/100	Novus Biologicals, CO, USA	[25]
Isl-1	Insulin Gene enhancer protein	Cardiomyocytes	polyclonal	1/100	Millipore, MA, USA	[26]
Anti-actinin	Anti- $\alpha$ -actinin	Cardiac muscle	AT6/172	1/200	Millipore, MA, USA	[27]
Anti-ANP	Atrial Natriuretic Peptide	Cardiomyocytes	23/1	1/200	Millipore, MA, USA	[28]
Anti-MHC	Myosin Heavy Chain	Skeletal Muscle cells	M5/114	1/200	Millipore, MA, USA	[29]
<b>Secondary Antibodies</b>						
Alexa fluor®-488 Goat anti-mouse				1/500	Invitrogen, CA, USA	
Alexa fluor®-546 Goat anti-rabbit				1/500	Invitrogen, CA, USA	

**Table 3.** Young's modulus, tensile strength, and percent elongation of PCL, PCL/TCNT fibers. Values were calculated using the Instron Bluehill® software.

<b>Material</b>	<b>Young's Modulus (MPa)</b>	<b>Tensile strength (MPa)</b>	<b>Elongation at break (%)</b>
PCL mesh	8.4	0.9	48
PCL/T-CNT mesh	11	1.3	131